SUPPLEMENTAL EXPERIMENTAL PROCEDURES AND FIGURES.

AS CDK8 Genome Editing

A TALEN pair was designed to generate a double-stranded break (DSB) 51 bp upstream of the F97 codon in exon 3 of CDK8, using TALEN Targeter (https://tale-nt.cac.cornell.edu/) (Cermak et al., 2011; Doyle et al., 2012) (Figure S1A). TALEN plasmids were constructed using the iterative capped assembly approach (Briggs et al., 2012), and verified by sequencing. To provide a template for homology-directed repair of the DSB while also stimulating homologous recombination, a recombinant adeno-associated virus (rAAV) donor construct was assembled using the pNeDaKO backbone (Kohli et al., 2004). The rAAV donor was comprised of ~900 bp homology arms adjoining a *loxP*-flanked neomycin-resistance cassette designed to insert 177 bp from codon 97, within the intron downstream of CDK8 exon 3 (Figure 1B, Figure S1). The right homology arm contained the base substitutions to create the F97G mutation (TTT > GGA), as well as adjacent silent changes to: (1) generate a novel *AvrII* restriction site to facilitate downstream validation; and (2) mutate the right TALEN site to prevent recognition of the edited allele by the TALEN pair (Figure S1B). The rationale for this arrangement was that homologous recombination events that repaired the DSB and included the neo^R cassette would also have incorporated the F97G and *AvrII* mutations within the intervening region, allowing efficient selection of the desired clones. The AAV Helper-Free System (Agilent) and associated plasmids were used to generate rAAV particles in AAV-293 packaging cells from the pNeDaKO-based CDK8-AS homology donor construct. Viral lysates were produced according to the manufacturer's directions and used as below to transduce HCT116 cells.

To generate the edits, parental HCT116 cells were transfected (Lipofectamine LTX, Life Technologies/Thermo Fisher Scientific) with plasmids encoding the TALEN pair, followed by rAAV infection and subsequent selection with G418 (Sigma Aldrich), and single-cell cloning. In the first round of editing we obtained heterozygous $CDK8^{as/wt}$ clones (Figure S1B, lanes 3 and 5) which were then pooled and subjected to Cre recombinase-mediated excision of the neo^R cassette. A second round of editing and selection was then carried out on this pool to target the second *CDK8* allele and obtain homozygous $CDK8^{as/as}$ clones (Figure S1B, lanes 2 and 4).

Initial screening of G418/neomycin-resistant clones was by PCR of genomic DNA using the following primers: CDK8-F1-fwd (5'-AGTGGTGGTGATCGCAGAAC-3') and CDK8-F1-rev (5'-TCTAGCCTTCGTCATGCCAC-3') to generate a 621 bp amplicon. PCR products amplified from mutant, but not WT *CDK8* alleles, possess a novel *AvrII* restriction site, generating two smaller fragments of 441 bp and 180 bp when digested (Figure S1B). Note that, because of the formation of undigestable heteroduplexes between WT and mutant products during PCR amplification, heterozygous clones only display ~25% digestion of the 621 bp product rather than the expected 50%, while 100% digestion is indicative of homozygous *CDK8*$^{as/as}$ clones.

To confirm the desired editing and integrity of the CDK8 exon 3 region, we further validated candidate clones by Southern blotting (Southern, 1975), using the 621 bp PCR product above as a probe. Exon 3 of *CDK8* is conveniently flanked by intronic *AvrII* sites 3.9 kb apart (Figure S1A). Genomic DNA (~15 µg) from WT and candidate *CDK8*$^{as/as}$ was digested to completion using *AvrII* (New England Biolabs). Following separation by agarose gel electrophoresis, the DNA was transferred to Nytran membrane (Whatman), using a Supercharge Turboblotter system (Whatman). Blocking, probe hybridization, and stringency washes were carried out according to the manufacturer's directions. The probe was labelled using a Detector PCR DNA Biotinylation Kit (KPL/Seracare) and streptavidin-conjugated alkaline phosphatase-based detection was performed with a Detector AP Chemiluminescent Blotting kit (KPL/ Seracare). Images were captured using an ImageQuant LAS4000 digital camera system (GE Healthcare).

Antibodies used for Western Blotting

CCNC: Bethyl A301-989A (1:500); CDK8: Santa Cruz Biotechnology sc-1521 (1:10,000); GLUT1: Abcam ab652 (1:1,000); GLUT3: Abcam ab191071 (1:1,000); HK1: Cell Signaling Technology #2024 (1:1,000); HIF1A: BD Transduction Laboratories 610959 (1:1,000); MED12: Bethyl A300-774A (1:500); MED14: Bethyl A301-044A (1:500); Nucleolin: Santa Cruz Biotechnology sc-8031 (1:10,000). STAT1: Santa Cruz Biotechnology sc-346 (1:1,000); STAT1-phospho-S727: Cell Signaling Technology #9177 (1:1,000); α-Tubulin: Sigma T9026 (1:20,000).

CDK8 Immunoprecipitation Kinase Assay

Cells (~1 x 10^7) were harvested in ice-cold PBS, resuspended in NP40-500 lysis buffer (100 mM Tris pH 7.5, 500 mM NaCl, 1% nonidet P-40 substitute (Source)) with protease inhibitors, and incubated on ice for 30 min. Lysates were sonicated briefly, cleared by centrifugation for 20 min at 20,000 rcf, and total protein quantified. For CDK8 immunoprecipitation, 9 mg of lysate was precleared by incubation with protein G sepharose beads (GE Healthcare) for 1 hr at 4°C. Fresh beads incubated with 5 µg of anti-CDK8 antibody (sc-1521) were then added to the supernatant, and incubated overnight at 4°C. The beads were then washed twice with 1 ml NP40-150 buffer (100 mM Tris pH 7.5, 150 mM NaCl, 1% nonidet P-40 substitute), four times with NP40-500 buffer, and twice more with NP40-150, followed by one wash and resuspension in 1 ml kinase buffer (25 mM Tris pH 7.5, 20 mM $MgCl_2$, 0.2 mM $NaVO_3$). A portion of this final material was removed for western blot analysis and 30% aliquots were spun down (2600 rcf) and resuspended in 30 µl of kinase buffer containing 3 µCi [γ-^{32}P]-ATP (Perkin Elmer) with either 10 µM of the ATP analogs 3MB-PP1 or 1NM-PP1 (Cayman Chemical), or the equivalent volume of vehicle (DMSO). After incubation for 30 min at 30°C, reactions were stopped by the addition of SDS-PAGE sample buffer and heated for 5 min at 95°C. Samples were then separated by SDS-PAGE, and the gel dried under vacuum at 60°C before exposure to a phosphor storage cassette and imaging using a STORM 860 scanner (Molecular Dynamics) at 100 µm resolution with Storm scanner control software (version 5.03). ImageJ and Photoshop were used to process the resulting data image and adjust contrast.

2D proliferation rate assay

HCT116 cells were seeded in 96-well plates 3,000 cells per well in McCoy's 5A containing drug or vehicle control. Growth rate was measured non-invasively in real time, using an IncuCyte Live Cell Imaging System (Essen Bioscience). For hypoxia treatments, plates were scanned once a day. The scanning time did not exceed 5 min and plates were returned to hypoxia immediately after the scan. The percentage of cell confluence was calculated as phase object confluence using the IncuCyte software.

3D Tumor Spheroid Growth Assay

HCT116 cells were seeded at 1,000 cells per well in 96-well ultra-low attachment plates (Corning) to form tumor spheroids. The growth rate of tumor spheroids was also monitored using the IncuCyte system, taking the average phase object area (μm^2) as determined by the IncuCyte software. Assuming each spheroid was perfectly spherical the surface area of each tumor spheroid was used to calculate the corresponding radius and volume. Growth kinetics of HCT116 tumor spheroids during treatment with 2DG (final concentration 2.5 mM, Alfa Aesar), Senexin A (final concentration 10 μM, Senexin A, Tocris Bioscience) and the combination of both drugs was monitored by IncuCyte imaging. Tumor spheroids were generated using 1 x 10^4 cells per well. Cells were allowed to form spheroids for 48 hrs, then 50% of medium (100 μl) was aspirated and replaced with 100μl of medium containing vehicle or drug, and incubated for a further 96 hrs.

Soft agar colony formation assay

HCT116 cells were counted and resuspended in 1 ml 0.5x McCoy's 5A with 0.4% w/v Noble agar (BD Difco), and plated in 6-well plates at 1 x 10^4 cells per well on top of a solidified layer of 2 ml 0.5x McCoy's 5A with 0.8% w/v Noble agar. After solidification for 10 min at room temperature, 2 ml of McCoy's 5A, supplemented with 10% fetal bovine serum and antibiotic-antimycotic mixture, was added to each well. Plates were incubated at 37°C for 21 days under 5% CO_2 (normoxia), or 21 days under 1% O_2, 5% CO_2 (hypoxia). At completion of the assay, media was removed and colonies were stained with 0.05% w/v Crystal Violet in 2% v/v methanol followed by destaining in 2% v/v methanol. Images of each plate were captured using an ImageQuant LAS4000 digital camera system (GE Healthcare) and colonies counted using ImageJ software (Schneider et al., 2012).

Xenograft growth assay in nude mice

HCT116 xenograft tumors were formed by subcutaneously injecting 2 x 10^6 cells (suspended in a 1:1 ratio of phosphate buffered saline:matrigel (growth factor-reduced, Corning)) into the left and right flanks of ten (five male, five female) six-week old athymic nude mice (Charles River strain 490) per group. Mice were monitored for tumor development/progression and euthanized three weeks after injection. Tumor volume

was measured with calipers several times per week, and calculated using the formula: volume = 0.5 x length x width^2.

Sulforhodamine B viability assay

Cell plating density was determined prior to the experiment depending on the cell size and proliferation rate of each cell line. HCT116 cells were seeded at 2500 cells per well, SW480 at 5000 per well, A549 at 4000 per well, H460 at 5000 cell per well, in media containing vehicle or drug. After 24 hrs incubation at 37°C, 5% CO_2, plates were incubated for a further 72 hrs at 37°C, 5% CO_2 (normoxia), or at 37°C, 1% O_2, 5% CO_2 (hypoxia), to give a total drug treatment time of 96 hrs. Cells were then fixed by addition of 10% Trichloroacetic acid (Thermo Fisher Scientific), and stained with 0.057% (w/v) Sulforhodamine B (SRB, MP Biomedicals) in 1% (w/v) acetic acid, according to the published protocol (Vichai and Kirtikara, 2006). Absorbance values (510 nm) were measured using a Synergy 2 plate reader (Biotek) and normalized to vehicle control within each condition and treatment.

RNA-seq library preparation and sequencing

Total RNA quality was assessed using Bioanalyzer RNA Pico chips (Agilent). PolyA RNA was purified from 15 µg total RNA using the Dynabeads mRNA Direct micro kit (Life Technologies/Thermo Fisher Scientific) according to the manufacturer's instructions, and ribosomal RNA contamination was assessed using Bioanalyzer RNA Pico chips (Agilent). Libraries for Ion Torrent sequencing were prepared using the Ion Total RNAseq v2 kit (Life Technologies/Thermo Fisher Scientific), according to the manufacturer's instructions. Yield and insert-size distribution were measured using Bioanalyzer High Sensitivity DNA chips (Agilent). The final Ion Torrent RNAseq libraries were subjected to an additional size-selection for 120-200 bp on a Blue Pippin (Sage Science) using a 2% dye-free gel with marker V1. Accounting for ~90 bp of Ion adapter sequences, this ensured a library insert size range of ~30-110 bp. Ion Torrent template preparation was carried out using the Ion PI Template OT2 200 Kit v2 and library sequencing was carried out on an Ion Torrent Proton sequencer using the Ion PI Sequencing 200 Kit v2 (Life Technologies/Thermo Fisher Scientific), according to the manufacturer's instructions.

RNA-seq data analysis

Signal processing, base-calling and removal of barcode and adapter sequences was carried out automatically by the Torrent Suite Software (Life Technologies/Thermo Fisher Scientific). Data quality was assessed using FASTQC (version 0.11.2, https://www.bioinformatics.babraham.ac.uk/projects/fastqc/) and FastQ Screen (version 0.11.0, https://www.bioinformatics.babraham.ac.uk/projects/fastq_screen/). Reads shorter than 30 nt were removed and long reads were trimmed to 150 nt using the Fastx toolkit. Alignment to the Human genome (hg19/GRCh37) was carried out using GSNAP (version 2015-06-12) (Wu and Nacu, 2010) with a mismatch setting of 3%. Reads with low mapping quality (MAPQ < 10) and multi-mapping reads were filtered using SAMtools (version 0.1.19) (Li et al., 2009), and Picard Tools (version 1.129, http://broadinstitute.github.io/picard/index.html) was used to sort reads by mapping position and mark duplicates. Gene-level counts were obtained using htseq-count (version 0.6.1) (Anders et al., 2015) using the GTF provided in the UCSC hg19-based igenomes bundle (https://support.illumina.com/sequencing/sequencing_software/igenome.html). Differential gene expression was assessed using DESeq2 (version 1.6.3) (Love et al., 2014) in R (version 3.1.0) with cutoffs as described in text and figure legends. Heat maps, bubble plots and volcano plots were made using the Python plotting library "matplotlib" (http://matplotlib.org/) and the R library "ggplot2" (http://ggplot2.org/). For visualization, bigwig tracks were prepared using deepTools (version 2.2.2, https://deeptools.github.io/) (--binSize=1 –minMappingQuality=10 --normalizeUsingRPKM).
RNA-seq data for CDK8 and CDK19 expression at the gene level was obtained from the European Molecular Biology Laboratory – European Bioinformatics Institute Gene Expression Atlas (https://www.ebi.ac.uk/gxa/experiments/E-MTAB-2706/) (Petryszak et al., 2016).

Analysis of Microarray data

Fluorescence data for HCT116 cells expressing non-targeting control (shControl), CDK8 (shCDK8), and CDK19 (shCDK19) shRNAs under normoxic and hypoxic conditions is available from Gene Expression Omnibus (GSE38061) (Galbraith et al., 2013). Data were $\log_2$ transformed and quantile normalized using

R version 3.3.3. Z-scores across all samples were calculated from mean values for replicates, and a heatmap was generated using the R package ComplexHeatmap version 1.12.0.

Analysis of TCGA data

TCGA (http://cancergenome.nih.gov/) level 3 RSEM V2 expression data was downloaded from the Broad TCGA GDAC Firehose (run 2016_01_28, doi:10.7908/C11G0KM9, http://gdac.broadinstitute.org/) using the 'firehose_get' download tool (https://confluence.broadinstitute.org/display/GDAC/Download), and imported to R version 3.3.3 for analysis. Spearman correlations were calculated for CDK8 and CDK19 paired with each glycolytic gene of interest using the R package Hmisc version 4.0-3. Boxplots were generated using the R package ggplot2 version 2.2.1, and sorted by median CDK8 correlation values. Heatmaps were generated using the R package ComplexHeatmap version 1.12.0, with rows (cancer types) and columns (genes) sorted by median CDK8 correlation values.

qRT-PCR Analysis of Gene Expression

Reverse transcription was carried out using a qScript cDNA synthesis kit (Quanta Biosciences). Quantitative PCR was carried out with reference to a standard curve using SYBR Select Master Mix for CFX (Life Technologies/Thermo Fisher Scientific) on a Viia7 Real-Time PCR system (Life Technologies/Thermo Fisher Scientific), and normalized to 18S rRNA signals. Primers used for qRT-PCR were as follows (5' to 3'):

18S-fwd, GCCGCTAGAGGTGAAATTCTTG; 18S-rev, CTTTCGCTCTGGTCCGTCTT; ENO1-fwd, GTCTCTTCAGGCGTGCAAGC; ENO1-rev, GATGAGACACCATGACGCCC; HK1-fwd, AGCAGACGCACAACAATGCCGT; HK1-rev, AAGTCACCATTCTCGGTCCCGT; SLC2A3-fwd, ATGGCCGCTGCTACTGGGTTTT; SLC2A3-rev, ACAACCGCTGGAGGATCTGCTT.

2NBDG Uptake Assay

Uptake of 2NBDG was measured as described previously (Yamada et al., 2007). Cells were plated at 8.3 x 10^3/well in 6-well plates and incubated for 72 hrs in normoxic or hypoxic conditions. 2-NBDG was added at final concentration of 50 μM to the medium. Control cells were not incubated with 2-NBDG. After 1 hr of incubation cells were washed once with PBS, then trypsinized and centrifuged for 5 min at

250 rcf. Cells were washed twice more with PBS and resuspended in 1 ml of PBS for flow cytometry (C6 Accuri Flow Cytometer, BD Bioscience) using 488 nm excitation a 533/30nm emission filter to measure 2-NBDG uptake. Data were normalized to constant cell number and analyzed using FlowJo software (Version 10.2).

Glycolysis Stress Test, ECAR and OCR Measurement

HCT116 cells at 5 x 10^4/well were plated in XF24 culture plates (Seahorse/Agilent) in McCoy's 5A medium and incubated for 24 hrs. Cells were then washed twice with PBS and incubated in glucose-free XF Assay Medium (Seahorse/Agilent) for 1 hr at 37°C and ambient CO_2 concentration, prior to running the assay. Injection ports were filled with solutions of glucose, oligomycin (VWR International Cat. 0215178605) and 2DG to give final concentrations of 50 mM, 1 µM, and 50 mM, respectively, in each well.

SUPPLEMENTAL REFERENCES

Anders, S., Pyl, P.T., and Huber, W. (2015). HTSeq--a Python framework to work with high-throughput sequencing data. Bioinformatics *31*, 166-169.

Briggs, A.W., Rios, X., Chari, R., Yang, L., Zhang, F., Mali, P., and Church, G.M. (2012). Iterative capped assembly: rapid and scalable synthesis of repeat-module DNA such as TAL effectors from individual monomers. Nucleic Acids Res *40*, e117.

Cermak, T., Doyle, E.L., Christian, M., Wang, L., Zhang, Y., Schmidt, C., Baller, J.A., Somia, N.V., Bogdanove, A.J., and Voytas, D.F. (2011). Efficient design and assembly of custom TALEN and other TAL effector-based constructs for DNA targeting. Nucleic Acids Res *39*, e82.

Doyle, E.L., Booher, N.J., Standage, D.S., Voytas, D.F., Brendel, V.P., Vandyk, J.K., and Bogdanove, A.J. (2012). TAL Effector-Nucleotide Targeter (TALE-NT) 2.0: tools for TAL effector design and target prediction. Nucleic Acids Res *40*, W117-122.

Galbraith, M.D., Allen, M.A., Bensard, C.L., Wang, X., Schwinn, M.K., Qin, B., Long, H.W., Daniels, D.L., Hahn, W.C., Dowell, R.D*., et al.* (2013). HIF1A Employs CDK8-Mediator to Stimulate RNAPII Elongation in Response to Hypoxia. Cell *153*, 1327-1339.

Kohli, M., Rago, C., Lengauer, C., Kinzler, K.W., and Vogelstein, B. (2004). Facile methods for generating human somatic cell gene knockouts using recombinant adeno-associated viruses. Nucleic Acids Res *32*, e3.

Li, H., Handsaker, B., Wysoker, A., Fennell, T., Ruan, J., Homer, N., Marth, G., Abecasis, G., Durbin, R., and Genome Project Data Processing, S. (2009). The Sequence Alignment/Map format and SAMtools. Bioinformatics *25*, 2078-2079.

Love, M.I., Huber, W., and Anders, S. (2014). Moderated estimation of fold change and dispersion for RNA-seq data with DESeq2. Genome Biol *15*, 550.

Petryszak, R., Keays, M., Tang, Y.A., Fonseca, N.A., Barrera, E., Burdett, T., Fullgrabe, A., Fuentes, A.M., Jupp, S., Koskinen, S.*, et al.* (2016). Expression Atlas update--an integrated database of gene and protein expression in humans, animals and plants. Nucleic Acids Res *44*, D746-752.

Schneider, C.A., Rasband, W.S., and Eliceiri, K.W. (2012). NIH Image to ImageJ: 25 years of image analysis. Nat Methods *9*, 671-675.

Southern, E.M. (1975). Detection of specific sequences among DNA fragments separated by gel electrophoresis. J Mol Biol *98*, 503-517.

Vichai, V., and Kirtikara, K. (2006). Sulforhodamine B colorimetric assay for cytotoxicity screening. Nat Protoc *1*, 1112-1116.

Wu, T.D., and Nacu, S. (2010). Fast and SNP-tolerant detection of complex variants and splicing in short reads. Bioinformatics *26*, 873-881.

Yamada, K., Saito, M., Matsuoka, H., and Inagaki, N. (2007). A real-time method of imaging glucose uptake in single, living mammalian cells. Nat Protoc *2*, 753-762.

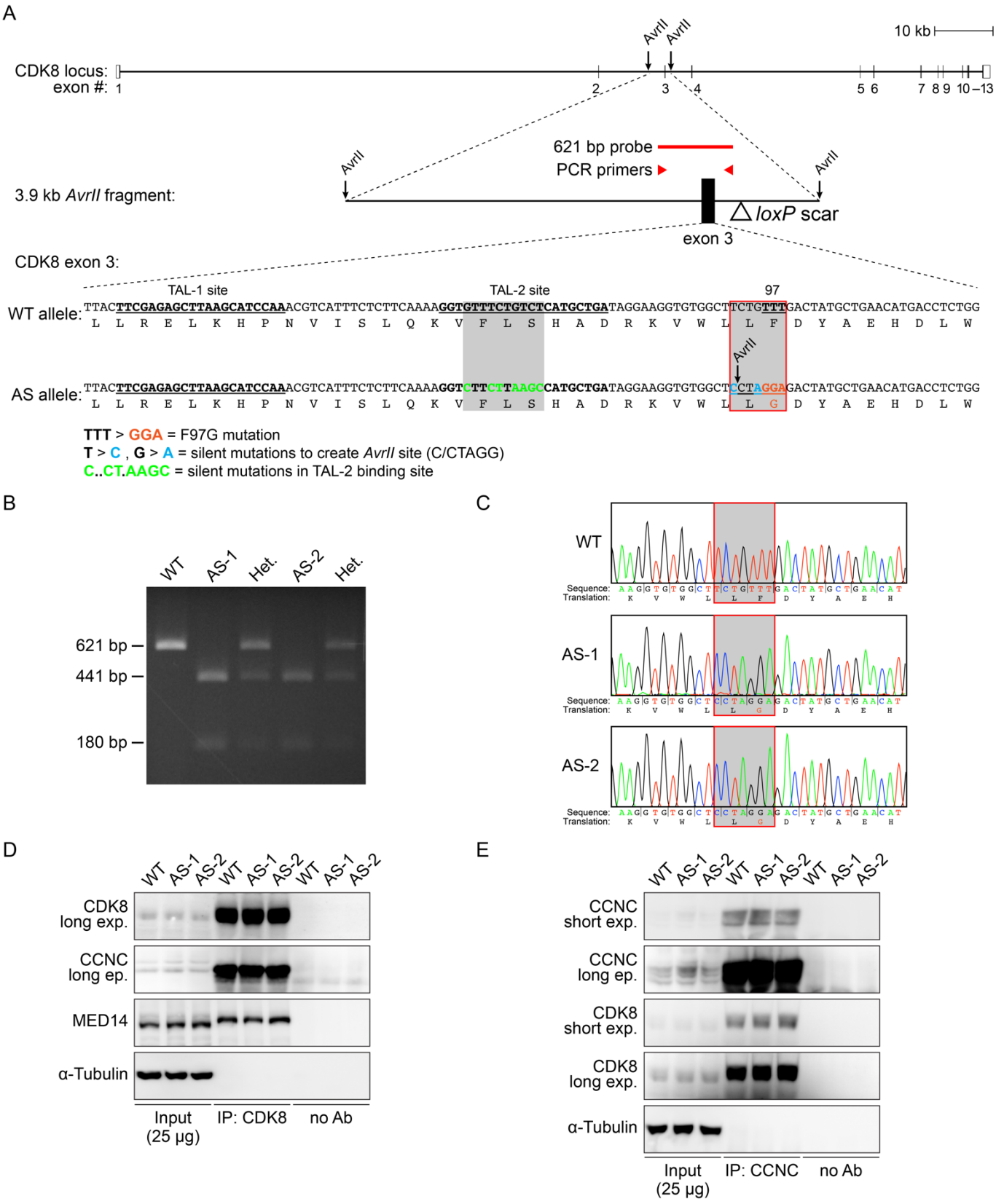

Figure S1, related to Figure 1. (A) Top: Schematic of the human *CDK8* locus indicating relative positions of exon 3 and flanking *AvrII* restriction sites. Middle: Map of the 3.9 kilo-base pair (kb) AvrII fragment showing size and positions of PCR primers, and the 621 base pair (bp) PCR product used for screening clones in B and as a probe for Southern blot hybridization. Bottom: Nucleotide and amino acids sequences for CDK8 exon 3 before (WT) and after (AS) editing. Recognition sites for the TALEN pair are underlined in bold (TAL-1 and TAL-2). Shaded boxes

highlight regions where changes were introduced. Colors denote the specific mutations for F97G (orange, non-synonymous), disruption of the TAL-2 site (green, silent), and creation of the novel *AvrII* restriction site adjacent to F97G (blue, silent). Shaded red box indicates region highlighted in C. (B) Ethidium bromide-stained agarose gel showing PCR products generated from genomic DNA taken from WT, homozygous CDK8$^{as/as}$ (AS-1 and AS-2), and heterozygous CDK8$^{wt/as}$ (Het.) HCT116 cells, using primers indicated in A, after overnight digestion with *AvrII*. The PCR product from WT cells does not possess an AvrII site, while 100% of products from homozygous clones will digest with *AvrII*, and products from heterozygotes represent a mixture of WT and *AvrII*-possessing fragments. Fragment sizes in base pairs are indicated at right. (C) Snaphots of sequencing traces for 621 base-pair PCR products for WT and two independent homozygous *CDK8*$^{as/as}$ clones (AS-1 and AS-2). Corresponding nucleotide and amino acid sequences are listed below traces. Shaded red boxes correspond to region highlighted in A. (D) Western blot analysis of CDK8 (long exposure to show input), Cyclin C (CCNC, long exposure to show input) and MED14 levels for inputs (2.5%) and CDK8 immunoprecipitations from WT and AS lysates. α-Tubulin included as loading control for input and as negative control for IP; no Ab, beads-only negative control. (E) Western blot analysis of Cyclin C (CCNC, long exposure to show input) and CDK8 (long exposure to show input) levels for inputs (2.5%) and Cyclin C immunoprecipitations from WT and AS lysates. α-Tubulin included as loading control for input and as negative control for IP; no Ab, beads-only negative control.

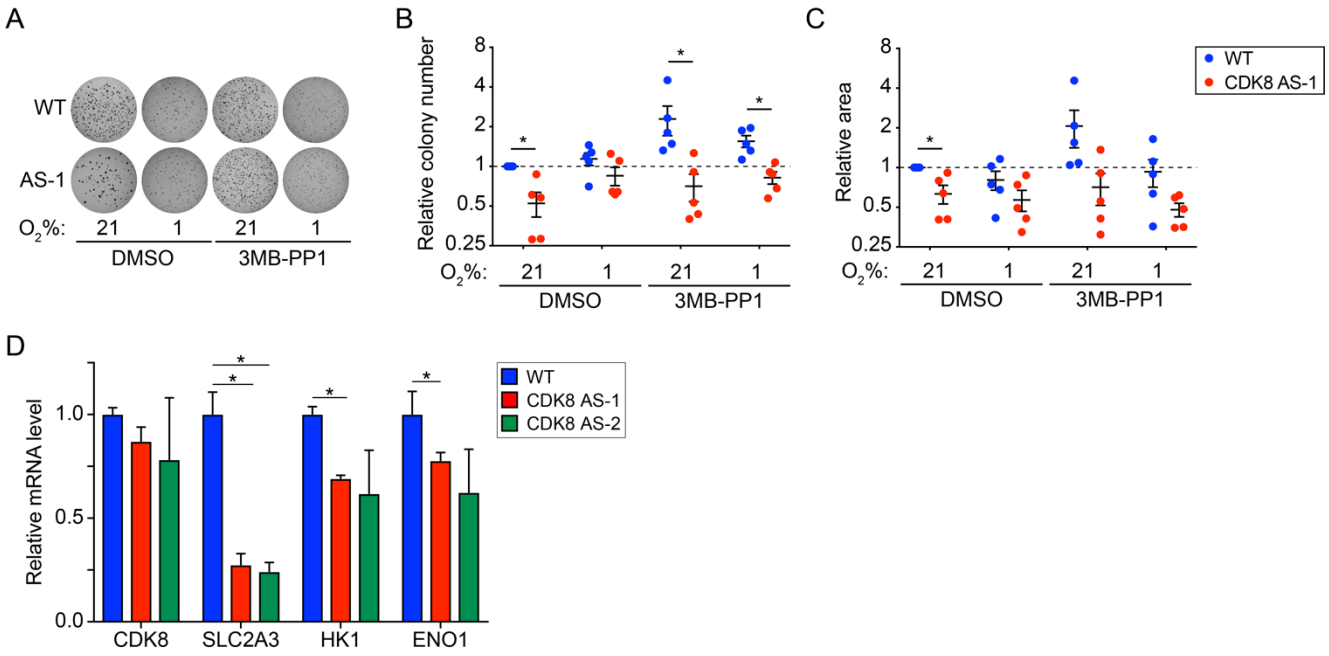

Figure S2, related to Figure 2. (A) Soft agar colony formation assay for WT and CDK8 AS-1 in normoxia and hypoxia (1% O_2), and treated with vehicle (DMSO) or 10 μM 3MB-PP1. Representative images shown. (B) Soft agar relative colony number for cells treated as in A. Individual replicates are shown as circles. Lines and whiskers represent mean ± SEM from five independent replicates. Asterisks indicate significant differences (unpaired t test, $p < 0.05$). (C) Soft agar relative colony area for cells treated as in A. Individual replicates are shown as circles. Lines and whiskers represent mean ± SEM from five independent replicates. Asterisks indicate significant differences (unpaired t test, $p < 0.05$). (D) Relative mRNA levels for *CDK8*, *SLC2A3*, *HK1*, and *ENO1* in HCT116 xenograft tumors, as assessed by qRT-PCR. Expression values were normalized to 18S ribosomal RNA and are expressed relative to the mean of wild-type samples. Data are represented as mean ± SEM from three individual tumors. Asterisks indicate significant differences (unpaired t test, $p < 0.05$).

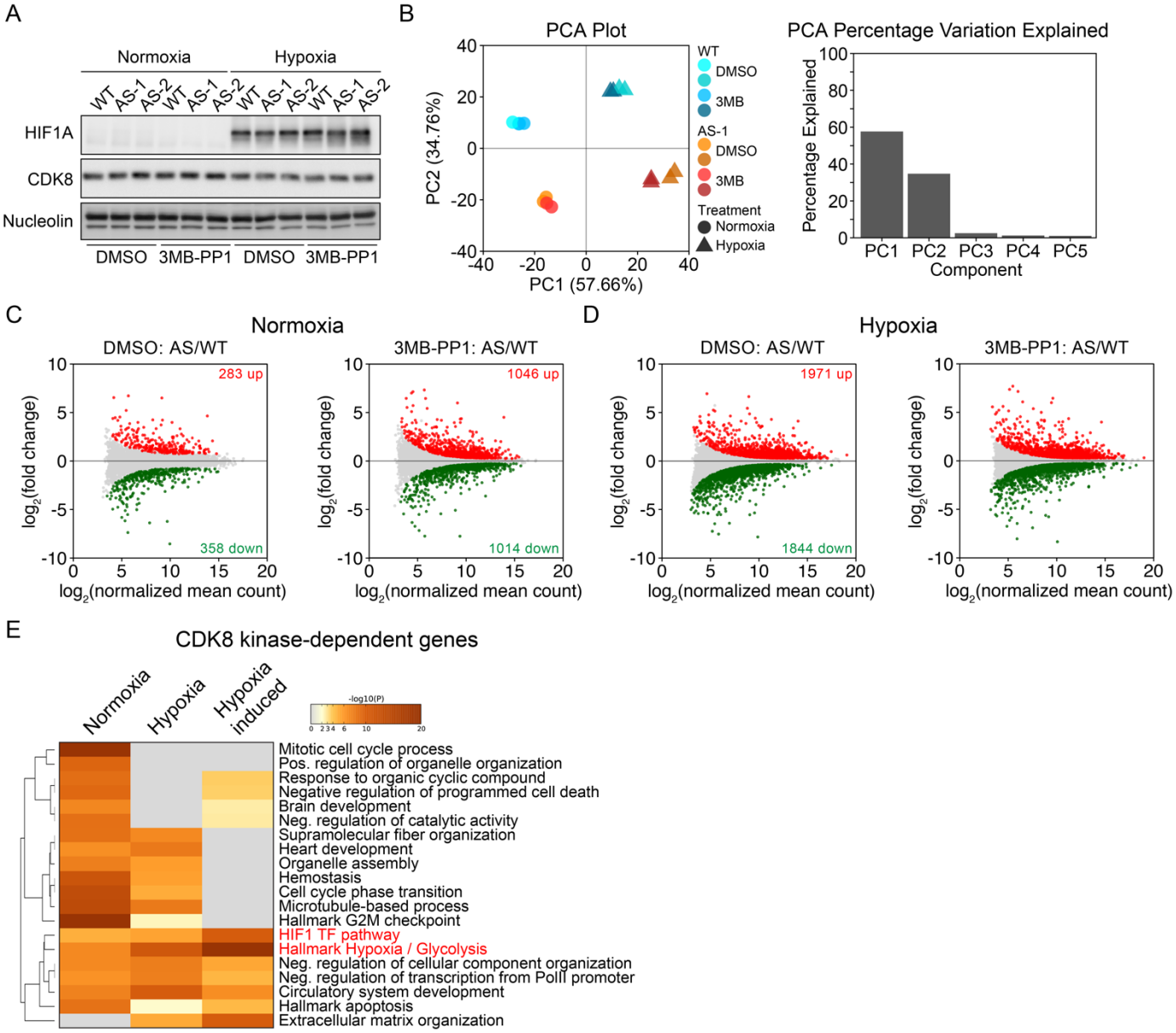

Figure S3, related to Figure 3. (A) Western blot showing levels of HIF1A and CDK8 in WT and two independent homozygous *CDK8*$^{as/as}$ clones (AS-1 and AS-2) in normoxia and hypoxia, treated with vehicle (DMSO) or 10 μM 3MB-PP1. (B) Principal component analysis of RNA-seq counts for the 500 genes with the highest variability across all samples. (C and D) MA plots (fold change vs. normalized mean count) for each comparison carried out using DESeq. Comparisons are indicated above each plot. Genes with significant changes (FDR adjusted p value <0.1) are colored red (increased expression) and green (decreased expression). (E) Top 20 clusters from Metascape comparison analysis of 1094 CDK8 kinase-dependent genes in normoxia, 2474 CDK8 kinase-dependent genes in hypoxia, and 292 CDK8 kinase-dependent hypoxia inducible genes. Color bars represents –$\log_{10}$(p value), based on the best-scoring term within each cluster. See also Table S1 and S2.

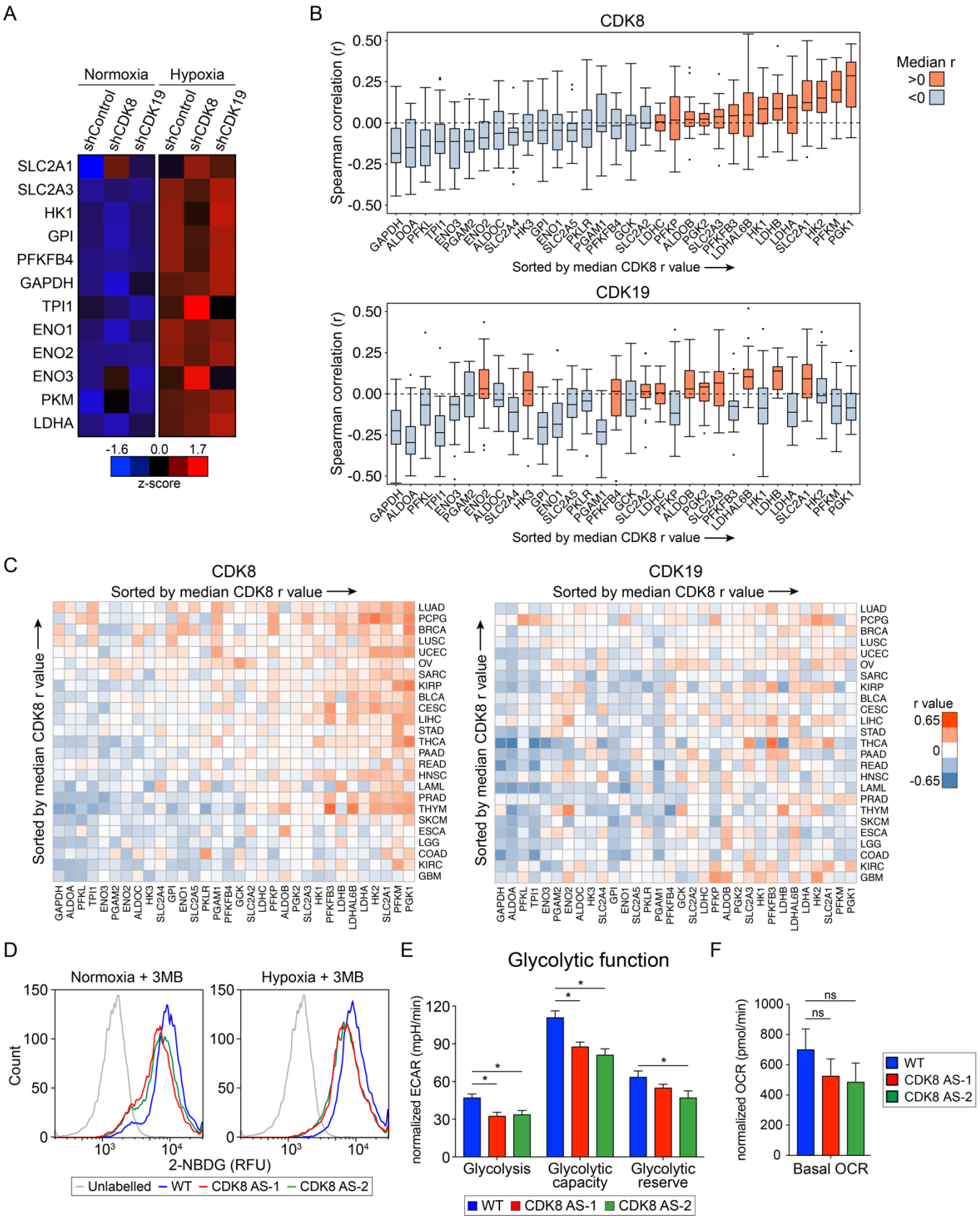

Figure S4, related to Figure 4. (A) Heatmap of microarray data showing relative expression of CDK8 kinase-dependent glycolytic genes in shControl, shCDK8, and shCDK19 HCT116 cells across normoxic and hypoxic conditions. Data are represented as z-scores of mean $\log_2$ quantile-normalized fluorescence values. (B) Boxplots of Spearman correlation values (r) across 25 cancer types for expression of CDK8 (top) or CDK19 (bottom) with each

of the listed glycolytic genes. Both plots are sorted by median r value for correlation with CDK8. Source data from TCGA. (C) Heatmaps of Spearman correlation values (r) for each of 25 cancer types for expression of CDK8 (left) or CDK19 (right) with each of the listed glycolytic genes. Columns and rows are sorted by median r value for CDK8 correlation for all columns or rows, respectively. Source data from TCGA. (D) Representative histograms of relative fluorescence for unlabeled vs. 2-NBDG-labelled WT and CDK8-AS-1 and -AS-2 cells in normoxic and hypoxic conditions, treated with 10 μM 3MB-PP1. (E) Glycolysis rate, capacity, and reserve derived from the extracellular acidification rate analysis in Figure 4H. Data are represented as mean ± SEM from five independent replicates. Asterisks indicate significant differences (unpaired t test, $p < 0.05$). (F) Basal oxygen consumption rate (OCR) of WT vs. CDK8-AS-1 and -AS-2 cells, measured after addition of glucose and before addition of oligomycin during glycolysis stress test. Data are represented as mean ± SEM from five independent replicates. No significant differences were detected (ns, unpaired t test, $p < 0.05$).

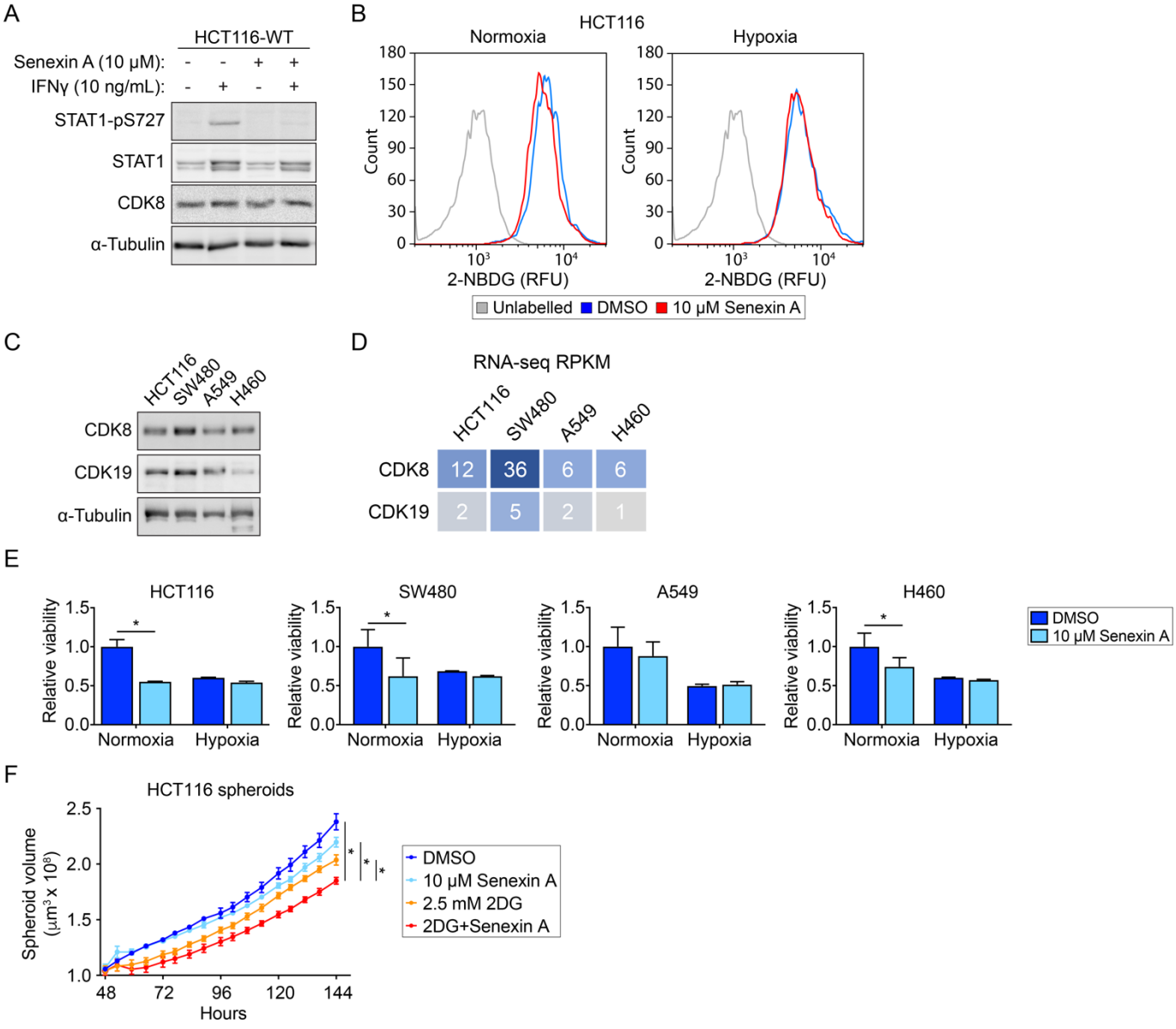

Figure S5, related to Figure 5. (A) Western blot showing levels of S727-phosphorylated STAT1 (STAT1-pS727), total STAT1, and CDK8 in HCT116 cell lysates following treatment with interferon gamma (IFNγ) and/or Senexin A. (B) Representative histograms of relative fluorescence for unlabeled vs. 2-NBDG-labelled HCT116 cells in normoxic and hypoxic conditions, treated with vehicle (DMSO) or 10 μM Senexin A. (C) Western blot showing relative expression levels of CDK8 and CDK19 protein in HCT116, SW480, A549, and H460 cells. (D) Gene level RNA-seq expression data (RPKM, reads per million per kb) for CDK8 and CDK19 in HCT116, SW480, A549, and H460 cells. Source data: EMBL-EBI Expression Atlas, experiment accession E-MTAB-2706. (E) Relative viability of HCT116, SW480, A549, and H460 cells grown under normoxic and hypoxic conditions, and treated with vehicle (DMSO) or 10 μM Senexin A. Data are represented as mean ± SEM from three independent replicates. Asterisks indicate significant differences (unpaired t test, $p < 0.05$). (F) Growth curves for HCT116 spheroids, treated with vehicle (DMSO), 10 μM Senexin A, 2.5 mM 2DG, or 10 μM Senexin A + 2.5 mM 2DG. Spheroid volume was calculated from area as monitored using an Incucyte imaging system. Data are represented as mean ± SEM from three independent replicates. Asterisks indicate significant differences (unpaired t test, $p < 0.05$).